We are IntechOpen, the world's leading publisher of Open Access books
Built by scientists, for scientists

4,800
Open access books available

122,000
International authors and editors

135M
Downloads

Our authors are among the

154
Countries delivered to

TOP 1%
most cited scientists

12.2%
Contributors from top 500 universities

CLARIVATE ANALYTICS
BOOK CITATION INDEX
INDEXED

WEB OF SCIENCE™

Selection of our books indexed in the Book Citation Index in Web of Science™ Core Collection (BKCI)

Interested in publishing with us?
Contact book.department@intechopen.com

Numbers displayed above are based on latest data collected.
For more information visit www.intechopen.com

29

Robust Inverse Filter Design Based on Energy Density Control

Junho Lee and Young-Cheol Park
Yonsei University
Korea

1. Introduction

3-D audio systems, which provide a listener with 3-D sound illusion at arbitrary locations, are an important part of immersive interfaces. 3-D audio systems can use headphones or loudspeakers to present the 3-D sound. A main limitation of producing 3-D sound through loudspeakers is distortion caused by room acoustics. Various methods of designing inverse filters that can equalize the room response have been suggested. One of the common problems of the previous methods is the restriction on the listener to sit in a relatively narrow equalization zone. The problems were mainly caused by the fact that equalization was conducted by controlling sound pressure at discrete points, and the points were not ideal locations to obtain global control of the pressure field.

Most inverse filtering approaches are based on the cost function defined by using acoustic pressure. These inverse filtering systems typically minimize the squared acoustic pressure at a control point using the least square (LS) optimization Nelson et al. (1992)Nelson et al. (1995)Kirkeby et al. (1998). These systems, however, often produce distortions such as boosting at certain frequencies in the vicinity of the control point, because the room transfer function (RTF), being defined in an acoustic pressure field, changes drastically with variation in source and receiver positions inside a space. Thus, a listener's slight movement easily harms the inverse filtering performance. To overcome the problem of distortion, an alternative equalization method called joint LS Abe et al. (1997)Ward (2000), was presented, in which a sum of the squared pressures at several control points is minimized. A major disadvantage of this approach is that global control over control points can be partly effective, sometimes; it is not guaranteed. Recently, the filters for crosstalk cancellation were designed using the minimax optimization Rao et al. (2007). The minimax approach is known to provide better channel separation in low-frequency than LS approach with marginal improvement Rao et al. (2007). But it still inherits the distortion problems mentioned previously, since it is also based on acoustic pressure at the control point.

Another approach to the problem of room transfer function (RTF) variations with source and receiver position is equalization via a vector quantization (VQ) method Mourjopoulos (1994), in which an inverse filter is updated during operation using an RTF codebook generated by using the VQ method. Although the inverse filtering using VQ methods can resolve the problems of previous methods by making them effective for all possible source and receiver positions inside the enclosure, the method needs large sets of off-line measurements of RTFs to make the RTF codebook and additional tracking modules to find receiver positions.

In this chapter, we present an alternative approach to the problem of room equalization. This approach utilizes a new performance function based on energy density. The idea of energy density control has been developed in the field of active noise control for the global attenuation of broadband noise fields Sommerfeldt & Nashif (1994). It was proven that the energy density control system outperforms the squared pressure system since the former system is capable of observing more modes of the pressure field in an enclosure than the latter. More specifically, if the magnitude of the potential energy in the form of pressure density associated with a particular mode goes to zero at a control point, the kinetic energy in the form of particle velocity will approach a maximum. Thus the algorithm is useful in widening the control zones. We will begin with reviewing the previous approaches to provide robust inverse filtering and their problems. Later, details of the energy density control will be described in application, such as in room equalization.

2. Inverse filtering for multichannel sound reproduction system

When a sound source generates a sound field in a room, a large number of echoes build up and then slowly decay as the sound is absorbed by the walls and the air, creating reverberation. It is a desirable property of auditoriums to the extent that it helps to overcome the inverse square law dropoff of sound intensity in the enclosure. However, if it is excessive, it makes the sounds run together with loss of articulation - the sound becomes muddy. In addition, they are also undesirable when reproducing a desired sound field in a room. A digital equalization filter can be used to compensate for deficiencies in a loudspeaker-room frequency response for sound reproduction systems. In order to design a sound reproduction system of this kind, one essentially has to invert the transfer function of the reproduction environment.

2.1 Previous approaches

2.1.1 Equalization based on joint LS optimization

Fig. 1 shows the general form of the inverse filtering network for controlling L points where $\mathbf{h}_{p,ml}(n), m = 1, \cdots, M, l = 1, \cdots, L, n = 0, \cdots, N_h - 1$, represents $N_h \times 1$ the acoustic impulse response vector of the path from the mth loudspeaker to the lth control point. To measure the acoustic impulse responses, in general, microphones are located at the control points and a test signal is radiated through loudspeakers. Thus, the impulse responses are obtained in the acoustic pressure field. Given the impulse responses, the objective of designing an equalization system is to find FIR filters $\mathbf{w}_m(n), n = 0, \cdots, N_w - 1$, such that the recorded signals are reproduced perfectly at the control points by making the equalized response as close as possible to the desired one.

The equalized response between the desired and actual impulse responses at the lth control point from M sources can be expressed as

$$\hat{d}_{p,l}(n) = \sum_{m=1}^{M} \sum_{k=0}^{N_h+N_w-2} w_m(k) h_{p,ml}(n-k), \ n = 0, \cdots, N_h + N_w - 1. \tag{1}$$

This can be written in a matrix form as

$$\hat{\mathbf{d}}_{p,l} = \begin{bmatrix} \mathbf{H}_{p,1l} & \mathbf{H}_{p,2l} & \cdots & \mathbf{H}_{p,Ml} \end{bmatrix} \begin{bmatrix} \mathbf{w}_1 \\ \mathbf{w}_2 \\ \vdots \\ \mathbf{w}_M \end{bmatrix}, \tag{2}$$

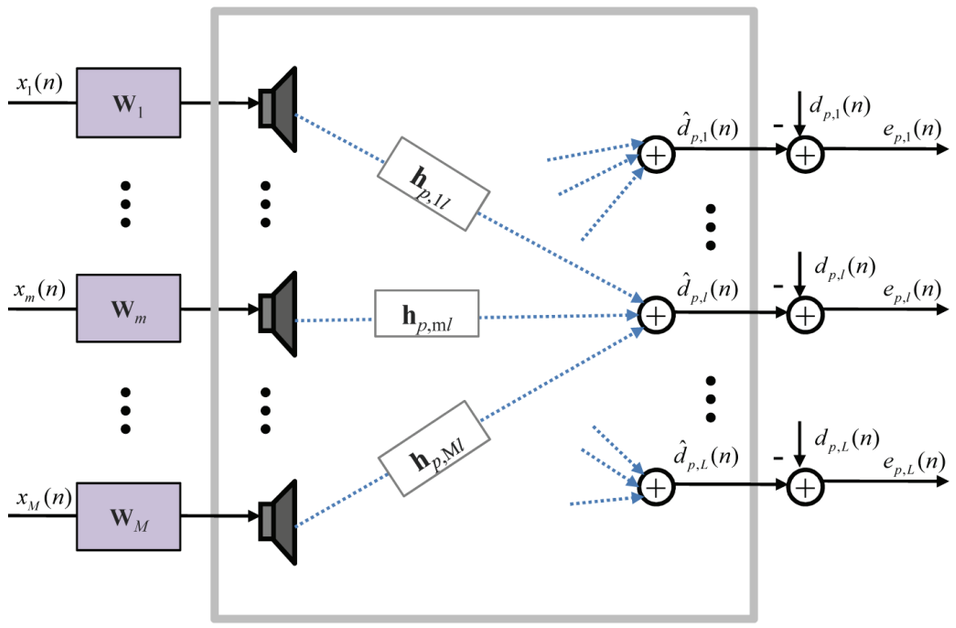

Fig. 1. Block diagram of the inverse filtering network.

where $\hat{\mathbf{d}}_{p,l} = [\hat{d}_{p,l}(0)\ \hat{d}_{p,l}(1)\ \cdots\ \hat{d}_{p,l}(N_h + N_w - 2)]^T$ is an $(N_h + N_w - 1) \times 1$ equalized response vector, $\mathbf{w}_m = [w_m(0)\ w_m(1)\ \cdots\ w_m(N_w - 1)]^T$ is an $N_w \times 1$ weight vector of the equalization filter, and the matrix $\mathbf{H}_{p,ml}$ is an $(N_h + N_w - 1) \times N_w$ convolution matrix defined using the acoustic impulse response as follows:

$$\mathbf{H}_{p,ml} = \begin{bmatrix} h_{p,ml}(0) & & 0 \\ \vdots & \ddots & \vdots \\ h_{p,ml}(N_h - 1) & \ddots & h_{p,ml}(0) \\ \vdots & \ddots & \vdots \\ 0 & & h_{p,ml}(N_h - 1) \end{bmatrix}. \tag{3}$$

Thus, the equalized response for M sound channels and L control points can be stacked as

$$\begin{bmatrix} \hat{\mathbf{d}}_{p,1} \\ \hat{\mathbf{d}}_{p,2} \\ \vdots \\ \hat{\mathbf{d}}_{p,L} \end{bmatrix} = \begin{bmatrix} \mathbf{H}_{p,11} & \mathbf{H}_{p,21} & \cdots & \mathbf{H}_{p,M1} \\ \mathbf{H}_{p,12} & \mathbf{H}_{p,22} & \cdots & \mathbf{H}_{p,M2} \\ \vdots & \vdots & \ddots & \vdots \\ \mathbf{H}_{p,1L} & \mathbf{H}_{p,2L} & \cdots & \mathbf{H}_{p,ML} \end{bmatrix} \begin{bmatrix} \mathbf{w}_1 \\ \mathbf{w}_2 \\ \vdots \\ \mathbf{w}_M \end{bmatrix} \tag{4}$$

or, more compactly as

$$\hat{\mathbf{d}}_p = \mathbf{H}_p \mathbf{w}. \tag{5}$$

The vector of error between the desired and actual impulse responses at the L control points can now be represented as

$$\mathbf{e}_p = \mathbf{d}_p - \mathbf{H}_p \mathbf{w} \tag{6}$$

where $\mathbf{d}_p = [\mathbf{d}_{p,1}^T \ \mathbf{d}_{p,2}^T \ \cdots \ \mathbf{d}_{p,L}^T]^T$ represent the desired impulse responses. Finally, an optimal weight vector can be obtained by minimizing the error between the desired and actual impulse responses. In an LS sense, the equalization filters are designed using a cost function:

$$J_{SP}(\mathbf{w}) = \left\| \mathbf{d}_p - \mathbf{H}_p \mathbf{w} \right\|_2 \tag{7}$$

where $\| \cdot \|_2$ denotes the vector 2-norm. The optimum set of coefficients in this case is given by

$$\mathbf{w}_{SP,o} = \mathbf{H}_p^+ \mathbf{d}_p \tag{8}$$

where $^+$ denotes pseudo inverse, so that $\mathbf{H}_p^+ = \left(\mathbf{H}_p^T \mathbf{H}_p \right)^{-1} \mathbf{H}_p^T$. Because the equalization filters in this case jointly minimize the sum of squared errors at the multiple control points, it is referred to as the joint LS method Ward (2000)Abe et al. (1997). Note that, for $L = 1$, the design method reduces to LS method Nelson et al. (1992)Nelson et al. (1995)Kirkeby et al. (1998).

The optimization method based on squared pressure is widely used because it guarantees to have a unique global minimum. However, it is found that the equalized response away from the error sensor position can be worse than the unequalized response in such a design method Elliott & Nelson (1989).

2.1.2 Equalization based on minimax optimization

An alternative approach to the design of equalization filters is to use minimax optimization techniques. Now, the cost function becomes

$$J_{PM}(\mathbf{w}) = \left\| \mathbf{d}_p - \mathbf{H}_p \mathbf{w} \right\|_\infty \tag{9}$$

where $\| \cdot \|_\infty$ denotes the L_∞ norm. It was originally proposed to design crosstalk cancellation filters Sturm (1999) but it can be applicable for designing equalization filters. The second-order cone programming (SOCP) approach can be used to design equalization filters in the minimax sense. The SOCP provides the optimization problem can be solved using interior point solvers such as the Self-Dual-Minimization (SeDuMi) toolbox of MATLAB Sturm (1999).

According to the results in Sturm (1999), the minimax approach gives better channel separation at low frequencies than the LS method. The same can be expected when it is used for the design of equalization filters, but it is also easily harmed by the movement of the listener's changes in location since this method inherits the robustness problem of equalization in the pressure field.

2.1.3 Equalization by vector quantization (VQ)

All-pole modeling of room responses can achieve reduction in the room transfer function (RTF) and the resulting equalizer order Mourjopoulos & Paraskevas (1991). According to this method, the all-pole model of the RTF with coefficients, $a_k, k = 1, 2, \cdots, K$, is defined as

$$H_{ap}(z) = \frac{G}{1 + \sum_{k=1}^{K} a_k z^{-k}} \tag{10}$$

where G is an arbitrary gain constant, K is the model order. And the following equation is the all-pole RTF equalizer's impulse response when $G = 1$:

$$w(n) = Z^{-1} \left[\frac{1}{H_{ap}(z)} \right]. \tag{11}$$

It is clear that an all-pole RTF equalizer will not achieve perfect equalization, because the all-pole model succeeds in representing poles of RTF, which correspond to resonances of RTF. This method, however, can achieve a required reduction in the equalizer order at some expense of its performance Toole & Olive (1988) and be used as the first stage of RTF processing at a second stage VQ . The use of vector quantization (VQ) can optimally classify such responses, obtained at different source and receiver positions Mourjopoulos (1994). Fig. 2 shows a block diagram for application of a VQ equalizer. By using the VQ method, the extremely large set of possible RTFs inside the enclosure will be classified into a smaller number of groups, so that a three-dimensional codebook of RTFs can be established, which can be used for equalizer design. During equalizer operation, the coefficients for equalization will be downloaded into the equalizer when it is detected that the listener is moving into a location. The combination of all-pole RTF modeling and the VQ method can solve the problems of the previous methods by making them effective for all possible source and receiver positions inside the enclosure.

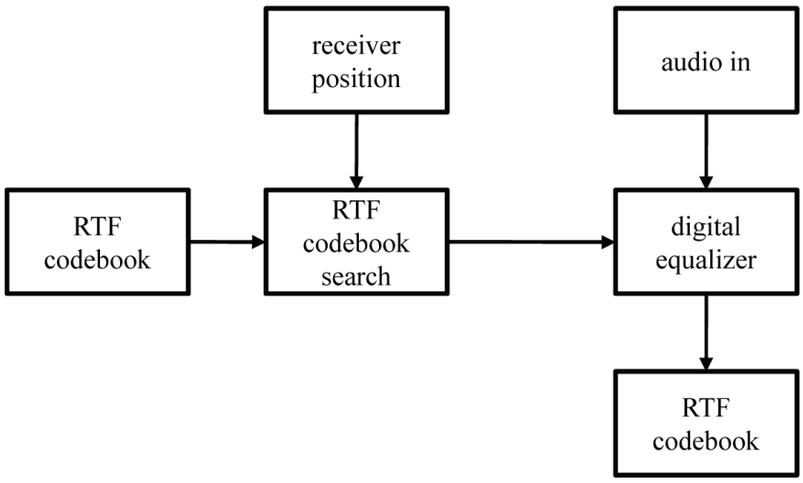

Fig. 2. Block diagram for application of VQ equalizer Mourjopoulos (1994).

2.2 Practical problems

As stated previously, most room equalization research is based on the cost function defined by using acoustic pressure and these equalization systems typically minimize the squared acoustic pressure at a control point using LS optimization Nelson et al. (1992)Nelson et al. (1995)Kirkeby et al. (1998)Abe et al. (1997)Ward (2000)Mourjopoulos (1994)Elliott & Nelson (1989). However, by controlling the acoustic pressure, the observability problem that leads to performance degradation happens. This is due to the magnitude of potential energy in the form of pressure associated with a particular mode goes to zero at the control point. Previous studies have shown that the geometry of the loudspeakers have a significant effect on the robustness of the inverse filtering Ward & Elko (1999). At certain frequencies, the sound signal arriving from the contralateral loudspeaker is delayed by approximately a half-period when compared with the signal coming from the ipsilateral loudspeaker. In a typical stereo setup with loudspeaker angle of 30° relative to the listener, the difference of the propagation path lengths between one loudspeaker and two listening points corresponding to the ear positions is $80 - 100mm$. Thus, in such a setup, one of the frequencies being involved in the signal cancellation is 1700Hz which corresponds to $190mm$ wavelength. At such frequencies,

the inverse filtering based on pressure control is associated with numerical problems that seriously impair the robustness of the control system. In Ward & Elko (1999), the effect of loudspeaker position on the robustness of crosstalk cancellers was analyzed and a simple expression for determining the optimum loudspeaker positions was derived.
On the other hand, the VQ method requires previous large sets of off-line measurements of RTFs in order to design the enclosure's codebook and an additional tracking module is necessary to deal with the listener's movement. In Gardner (1997), Gardner employed a head tracking module using a camera in order to solve the performance degradation of the binaural synthesizer and the crosstalk canceller being caused by head movement. Fig. 3 shows a head-tracked 3-D loudspeaker audio system. The binaural synthesis block is to synthesize the ear signals corresponding to the target scene by appropriately encoding directional cues, and the crosstalk cancellation network delivers these signals to the listener without distortions by inverting the acoustic impulse response of the path from loudspeakers to the listener. When the listener moves away from the listening point, the crosstalk canceller and the binaural synthesis module are steered to the location of the tracked listener with the help of the head tracker module. In such a way, the 3-D audio system can preserve the 3-D illusion over a large listening area.

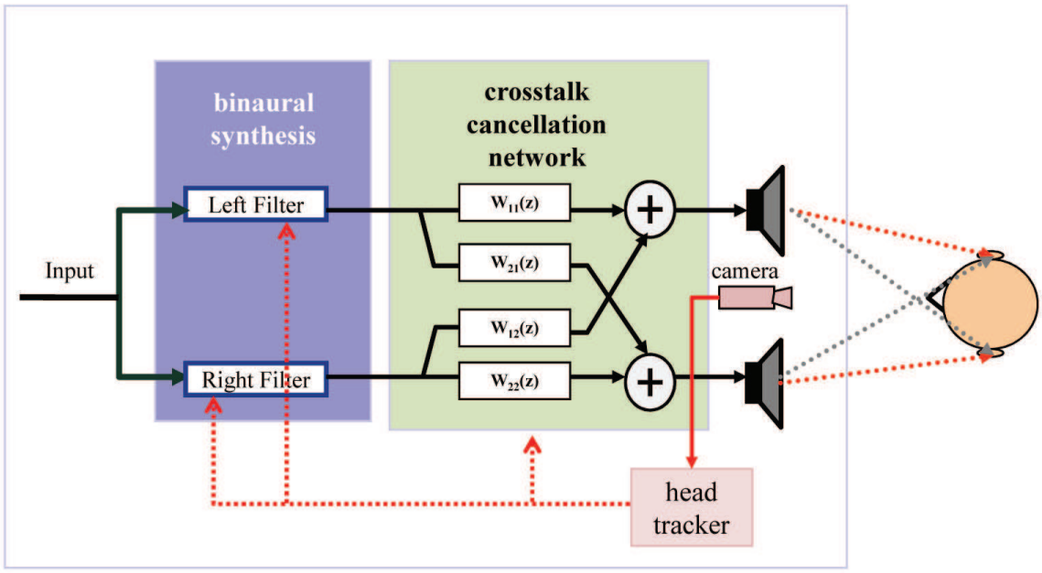

Fig. 3. Block diagram of head-tracked 3-D loudspeaker audio system.

3. Robust inverse filtering for multichannel sound reproduction system

Acoustic energy density function is defined using acoustic pressure and particle velocity. By controlling acoustic energy density, the observability problems that often limit the performance when controlling the pressure field are effectively overcome. To control acoustic energy density, however, a velocity sensor or equivalent estimation method is required.

3.1 Acoustic energy density

The time-averaged acoustic energy density at a point in space, $\mathbf{x} = (x, y, z)$, is defined as

$$\xi(\mathbf{x}) = \frac{1}{4\rho c^2} |p(\mathbf{x})|^2 + \frac{\rho}{4} |\vec{v}(\mathbf{x})|^2 \tag{12}$$

where ρ is the ambient fluid density, c is the acoustic wave speed, $p(\mathbf{x})$ is the acoustic pressure, and $\vec{v}(\mathbf{x}) = (v_x(\mathbf{x}), v_y(\mathbf{x}), v_z(\mathbf{x}))$ is the acoustic velocity vector. Note that acoustic energy density consists of potential energy density in the form of pressure and kinetic energy density in the form of particle velocity. Thus, it can be said that systems based on the squared pressures use only half of the acoustic information. Minimizing the sum of the squared pressure, which is part of the potential energy, at discrete points in space may significantly increase both the kinetic energy at those points as well as the total energy in the enclosure. The squared pressure system therefore often yields only local control. On the other hand, minimizing the sum of the total energy density at discrete points can yield improved equalization over a wide area covered by the control points since the energy has been definitely reduced at least at the specified points in space Parkins et al. (2000).

As previously mentioned, the acoustic pressure-based control inherently suffers from the observability problem that limits performance. One way of overcoming this problem is to control the acoustic energy density that is expected to provide robust equalization due to fairly uniform distribution of acoustic energy density.

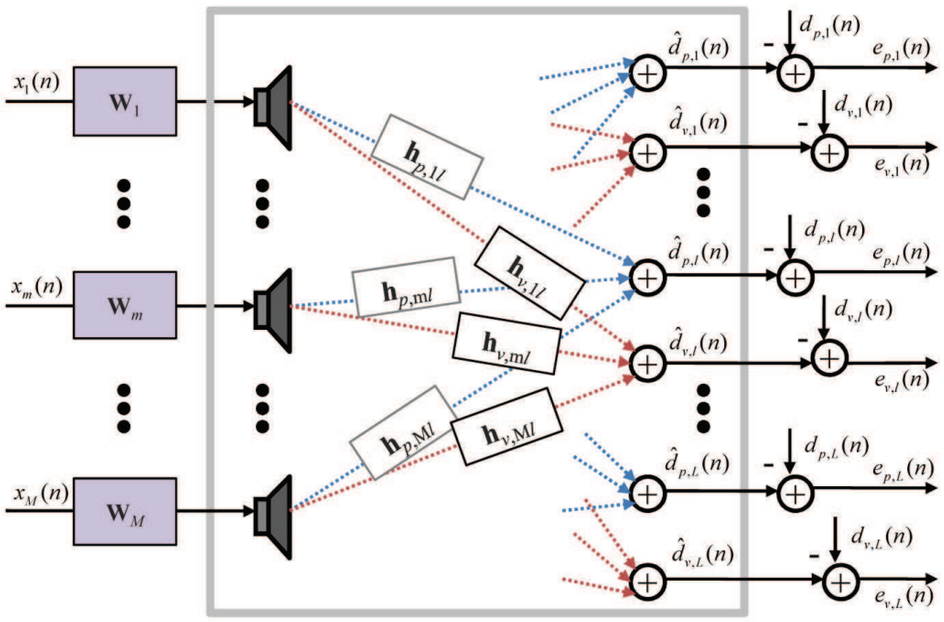

Fig. 4. Block diagram of the inverse filtering based on energy density control.

3.2 Equalization based on energy density control

Fig. 4 shows a block diagram of the inverse filtering system with L control points. The acoustic impulse responses in the velocity field at the lth control point due to M sources are described as

$$\hat{d}_{v_x,l}(n) = \sum_{m=1}^{M} \sum_{k=0}^{N_h+N_w-2} w_m(k) h_{v_x,ml}(n-k), \tag{13}$$

$$\hat{d}_{v_y,l}(n) = \sum_{m=1}^{M} \sum_{k=0}^{N_h+N_w-2} w_m(k) h_{v_y,ml}(n-k), \tag{14}$$

$$\hat{d}_{v_z,l}(n) = \sum_{m=1}^{M} \sum_{k=0}^{N_h+N_w-2} w_m(k) h_{v_z,ml}(n-k), \tag{15}$$

where the subscript v_x, v_y, and v_z refer to the x, y, and z-directional components of velocity, respectively. Let $\hat{\mathbf{d}}_{v,l}^T$ and $\mathbf{H}_{v,ml}$, respectively, denote the 3×1 velocity vector and $3(N_h + N_w - 1) \times N_w$ convolution matrix as given by

$$\hat{\mathbf{d}}_{v,l}^T = \left[\hat{d}_{v_x,l}(n) \ \hat{d}_{v_y,l}(n) \ \hat{d}_{v_z,l}(n) \right]^T, \tag{16}$$

$$\mathbf{H}_{v,ml} = \begin{bmatrix} \mathbf{H}_{v_x,ml} \\ \mathbf{H}_{v_y,ml} \\ \mathbf{H}_{v_z,ml} \end{bmatrix}. \tag{17}$$

The elements $\mathbf{H}_{v_x,ml}$, $\mathbf{H}_{v_y,ml}$, and $\mathbf{H}_{v_z,ml}$ are matrices defined similarly to Eq. (3). Now, the equalized velocity response at the control point l can be written as

$$\hat{\mathbf{d}}_{v,l}^T = \left[\mathbf{H}_{v,1l} \ \mathbf{H}_{v,2l} \ \cdots \ \mathbf{H}_{v,Ml} \right] \begin{bmatrix} \mathbf{w}_1 \\ \mathbf{w}_2 \\ \vdots \\ \mathbf{w}_M \end{bmatrix}. \tag{18}$$

The equalized velocity responses can be stacked in a matrix as

$$\begin{bmatrix} \hat{\mathbf{d}}_{v,1} \\ \hat{\mathbf{d}}_{v,2} \\ \vdots \\ \hat{\mathbf{d}}_{v,L} \end{bmatrix} = \begin{bmatrix} \mathbf{H}_{v,11} & \mathbf{H}_{v,21} & \cdots & \mathbf{H}_{v,M1} \\ \mathbf{H}_{v,12} & \mathbf{H}_{v,22} & \cdots & \mathbf{H}_{v,M2} \\ \vdots & \vdots & \ddots & \vdots \\ \mathbf{H}_{v,1L} & \mathbf{H}_{v,2L} & \cdots & \mathbf{H}_{v,ML} \end{bmatrix} \begin{bmatrix} \mathbf{w}_1 \\ \mathbf{w}_2 \\ \vdots \\ \mathbf{w}_M \end{bmatrix} \tag{19}$$

or

$$\hat{\mathbf{d}}_v = \mathbf{H}_v \mathbf{w}. \tag{20}$$

Now, the vector of error between the desired and equalized responses in the velocity field at the L control points is given as

$$\mathbf{e}_v = \mathbf{d}_v - \mathbf{H}_v \mathbf{w} \tag{21}$$

where $\mathbf{d}_v = [\mathbf{d}_{v,1}^T \ \mathbf{d}_{v,2}^T \ \cdots \ \mathbf{d}_{v,L}^T]^T$ represent desired impulse responses in velocity fields. Using Eqs. (6) and (21), the acoustic energy density at the control points is expressed as

$$\xi = \frac{1}{2\rho c^2} \left[\mathbf{e}_p^T \mathbf{e}_p + (\rho c)^2 \mathbf{e}_v^T \mathbf{e}_v \right]. \tag{22}$$

For controlling the energy density, the optimal weight vector is determined by the following cost function:

$$J_{ED}(\mathbf{w}) = \left\| \begin{bmatrix} \mathbf{d}_p \\ (\rho c)\, \mathbf{d}_v \end{bmatrix} - \begin{bmatrix} \mathbf{H}_p \mathbf{w} \\ (\rho c)\, \mathbf{H}_v \mathbf{w} \end{bmatrix} \right\|_2. \tag{23}$$

Note that the modified energy density, i.e. $(2\rho c^2)\xi$, is chosen as the cost function. The optimum filter coefficients are then

$$w_{ED,o} = \begin{bmatrix} \mathbf{H}_p \\ (\rho c)^2 \mathbf{H}_v \end{bmatrix}^+ \begin{bmatrix} \mathbf{d}_p \\ (\rho c)^2 \mathbf{d}_v \end{bmatrix}. \tag{24}$$

3.3 Velocity components estimation

As shown in Eq. (19), we need the x, y, and z-components of the acoustic velocity to implement the energy density control method. To this end, we can use a particle velocity sensor such as a laser vibrometer or velocity microphone. But a more convenient method of doing the same is approximated estimation using two pressure sensors (microphones). In this method, it is assumed that two microphones are highly phase-matched.
Euler's equation in one dimension relates the gradient of the acoustic pressure to the time-derivative of the acoustic velocity at a point as

$$\rho \frac{\partial v_x(x,t)}{\partial t} = -\frac{\partial p(x,t)}{\partial x}. \tag{25}$$

Thus, the acoustic velocity is obtained using

$$\hat{v}_x(x,t) = -\frac{1}{\rho}\int_{-\infty}^{t} \frac{\partial p(x,t)}{\partial x} dt. \tag{26}$$

By approximating the pressure gradient as the pressure difference in a small distance, Eq. (35) can be approximated as

$$\hat{v}_x(x,t) \approx -\frac{1}{\rho}\int_{-\infty}^{t} \frac{p_2(t) - p_1(t)}{\Delta x} dt \tag{27}$$

where $p_1(t)$ and $p_2(t)$ are the pressures measured by two closely spaced microphones with a distance Δx. Integration can be performed using a digital integrator Hodges et al. (1990) expressed in a simple recursive form:

$$\hat{v}_x(n) = \hat{v}_x(n-1) - \frac{1}{\rho \Delta x f_s}\left[p_2(n) - p_1(n)\right] e^{-1/f_s} \tag{28}$$

where f_s denotes the sampling frequency.

3.4 Robustness analysis

For ease of analysis, we define the transfer function (TF) between the mth loudspeaker and the lth control point as Ward & Elko (1999)

$$\mathcal{H}_{p,ml}(\omega) = e^{j2\pi\lambda^{-1}\Delta_{ml}}, \tag{29}$$

where λ is the wavelength and Δ_{ml} is the distance between the loudspeaker and the control point. It should be noted that this model disregards both propagation attenuation and the head shadow effect. Assuming a transaural system, the transfer functions between the two loudspeakers and the two microphones are collectively expressed as

$$\mathbb{H}_p(\omega) = \begin{bmatrix} \mathcal{H}_{p,11}(\omega) & \mathcal{H}_{p,12}(\omega) \\ \mathcal{H}_{p,21}(\omega) & \mathcal{H}_{p,22}(\omega) \end{bmatrix}. \tag{30}$$

Then the robustness of the equalization system is reflected by the condition number of the matrix $\mathbb{H}_p(\omega)$ Ward & Elko (1999) defined as

$$cond\left\{\mathbb{H}_p(\omega)\right\} = \frac{\sigma_{\max}\left(\mathbb{H}_p^H(\omega)\mathbb{H}_p(\omega)\right)}{\sigma_{\min}\left(\mathbb{H}_p^H(\omega)\mathbb{H}_p(\omega)\right)}, \tag{31}$$

where $\sigma_{min}(\cdot)$ and $\sigma_{max}(\cdot)$ denote the smallest and largest singular values, respectively. Suppose that the TF matrix is acoustically symmetric so that $\mathcal{H}_{p,11}(\omega) = \mathcal{H}_{p,22}(\omega)$ and $\mathcal{H}_{p,21}(\omega) = \mathcal{H}_{p,12}(\omega)$. We now have

$$\mathbb{H}_p^H(\omega)\mathbb{H}_p(\omega) = 2\left|\mathcal{H}_{p,11}(\omega)\right|^2 \begin{bmatrix} 1 & \cos(2\pi\lambda^{-1}\Delta) \\ \cos(2\pi\lambda^{-1}\Delta) & 1 \end{bmatrix}, \tag{32}$$

where Δ denotes the interaural path difference given by $\Delta_{11} - \Delta_{12}$. Singular values can be found from the following characteristic equation:

$$(1-k)^2 - \cos^2(2\pi\lambda^{-1}\Delta) = 0. \tag{33}$$

By the definition of robustness, the equalization system will be the most robust when $\cos(2\pi\lambda^{-1}\Delta) = 0$ ($\mathbb{H}_p(\omega)$ is minimized) and the least robust when $\cos(2\pi\lambda^{-1}\Delta) = \pm 1$ ($\mathbb{H}_p(\omega)$ is maximized) Ward & Elko (1999).

A similar analysis can be applied to acoustic energy density control. The composite transfer function between the two loudspeakers and the two microphones in the pressure and velocity fields becomes

$$\mathbb{H}_{ed}(\omega) = \begin{bmatrix} \mathcal{H}_{p,11}(\omega) & \mathcal{H}_{p,21}(\omega) \\ (\rho c)\mathbb{H}_{v,11}(\omega) & (\rho c)\mathbb{H}_{v,21}(\omega) \\ \mathcal{H}_{p,12}(\omega) & \mathcal{H}_{p,22}(\omega) \\ (\rho c)\mathbb{H}_{v,12}(\omega) & (\rho c)\mathbb{H}_{v,22}(\omega) \end{bmatrix}, \tag{34}$$

where $\mathbb{H}_{v,ml}(\omega)$ is the frequency-domain matrix corresponding to $\mathbf{H}_{v,ml}$. Note that the pressure and velocity at a point in space $\mathbf{x} = (x, y, z)$, $\overrightarrow{v}(\mathbf{x})$, and $p(\mathbf{x})$ are related via

$$j\omega\rho\,\overrightarrow{v}(\mathbf{x}) = -\nabla p(\mathbf{x}), \tag{35}$$

where ∇ represents a gradient. Using this relation, the velocity component for the x direction can be written as

$$\mathcal{H}_{v_x,ml}(\omega) = \frac{1}{\rho c} \cdot \frac{\Delta x_{ml}}{d}\mathcal{H}_{p,ml}(\omega), \tag{36}$$

where d and Δx_{ml} denote the distance and the x component of the displacement vector between the mth loudspeaker and the lth control point, respectively. Note that the velocity component for the y and z directions can be expressed similarly. Now we have

$$\mathbb{H}_{ed}^H(\omega)\mathbb{H}_{ed}(\omega) = 2\begin{bmatrix} 2 & Q\cos(2\pi\lambda^{-1}\Delta) \\ Q\cos(2\pi\lambda^{-1}\Delta) & 2 \end{bmatrix}, \tag{37}$$

where

$$Q = 1 + \frac{\Delta x_{11}\Delta x_{12} + \Delta y_{11}\Delta y_{12} + \Delta z_{11}\Delta z_{12}}{d_{11}(d_{11}+\Delta)}. \tag{38}$$

Singular values can be obtained from the following characteristic equation:

$$(2-k)^2 - \left(Q\cos\left(2\pi\lambda^{-1}\Delta\right)\right)^2 = 0. \tag{39}$$

From Eqs. (33) and (39), it can be noted that the maximum condition number of $\mathbb{H}_p(\omega)$ equals to infinity, while that of $\mathbb{H}_{ed}(\omega)$ is $(2+Q)/(2-Q)$, when $\cos(2\pi\lambda^{-1}\Delta) = \pm 1$. Eq. (38) also shows that the maximum condition number of the energy density field becomes smaller as Δ increases because Q approaches to 1. Now, by comparing the maximum condition numbers,

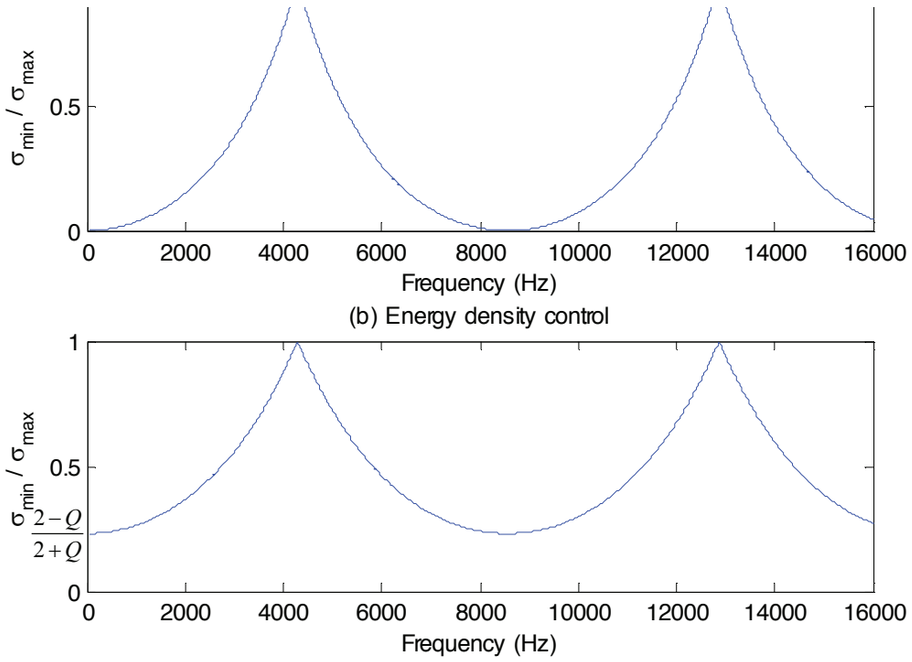

Fig. 5. The reciprocal of the condition number.

the robustness of the control system can be inferred. Fig. 5 shows the reciprocal condition number for the case where the loudspeaker is symmetrically placed at a 1 m and 30° relative to the head center. The reciprocal condition number of the pressure control approaches to zero, but the energy density control has the reciprocal condition numbers that are relatively significant for entire frequencies. Thus, it can be said that the equalization in the energy density field is more robust than the equalization in the pressure field.

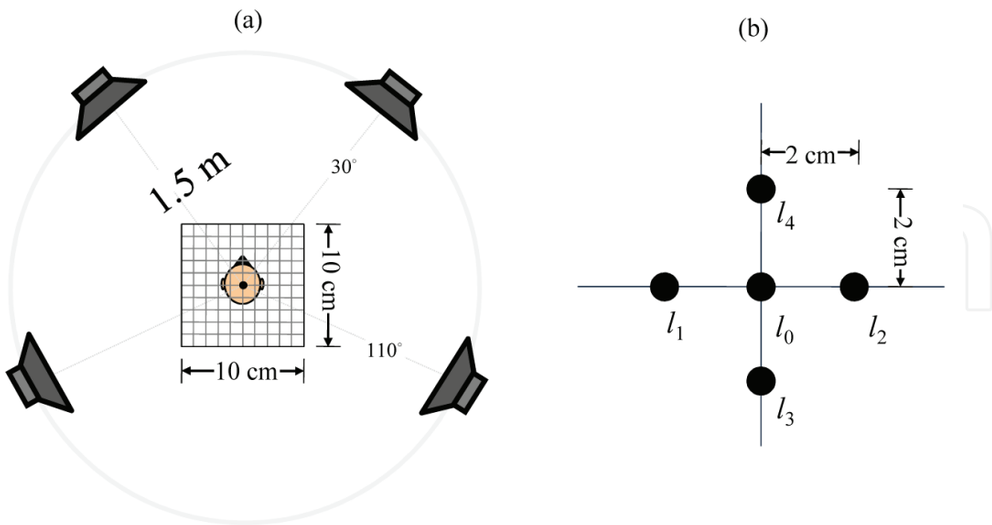

Fig. 6. Simulation environments. (a) Configuration for the simulation of a multichannel sound reproduction system. (b) Control points in the simulations. l_0 corresponds to the center of the listener's head.

4. Performance Evaluation

We present simulation results to validate energy density control. First, the robustness of an inverse filtering for multichannel sound reproduction system is evaluated by simulating the acoustic responses around the control points corresponding to the listener's ears. The performance of the robustness is objectively described in terms of the spatial extent of the equalization zone.

4.1 Simulation result

In this simulation, we assumed a multichannel sound reproduction system consisting of four sound sources ($M = 4$) as shown in Fig. 6(a). Details of the control points are depicted in Fig. 6(b). We assumed a free field radiation and the sampling frequency was 48 kHz. Impulse responses from the loudspeakers to the control points were modeled using 256-tap FIR filters ($N_h = 256$), and equalization filters were designed using 256-tap FIR filters ($N_w = 256$). The conventional LS method was tried by jointly equalizing the acoustic pressure at l_1, l_2, l_3, and l_4 points, and the energy density control was optimized only for the l_0 point. The delayed Dirac delta function was used for the desired response, i.e., $d_{p,l_0}(n) = \cdots = d_{p,l_4}(n) = \delta(n - n_0)$.

Center frequency	The control point (cm)				
	(0, 0)	(0, 5)	(2.5, 2.5)	(5, 0)	(5, 5)
500 Hz	0.06	-0.28	-0.13	-0.42	-0.28
1 kHz	0.30	-1.39	-0.60	-1.91	-3.55
2 kHz	1.26	-7.61	-2.76	-14.53	-10.25

Table 1. The error in dB for the pressure control system based on joint LS optimization at each center frequency.

Center frequency	The control point (cm)				
	(0, 0)	(0, 5)	(2.5, 2.5)	(5, 0)	(5, 5)
500 Hz	0.00	0.25	0.09	-0.21	0.03
1 kHz	0.00	0.25	0.06	-0.95	-0.76
2 kHz	0.00	0.25	-0.69	-4.50	-4.58

Table 2. The error in dB for the energy density control system at each center frequency.

We scanned the equalized responses in a 10 cm square region around the l_0 position, and results are shown in Fig. 7. Note that only the upper right square region was evaluated due to the symmetry. For the energy density control, velocity x and y were used. Velocity z was not used. As evident in Fig. 7, the energy density control shows a lower error level than the joint LS-based squared pressure control over the entire region of interest except at the points corresponding to l_2 $(2\ cm, 0\ cm)$ and l_4 $(0\ cm, 2\ cm)$, where the control microphones for the joint LS control were located.

Next, an equalization error was measured as the difference between the desired and actual responses defined by

$$C(dB) = 10 \log \left\{ \frac{\sum_{\omega=\omega_{min}}^{\omega_{max}} \left| \mathcal{D}(\omega) - \hat{\mathcal{D}}(\omega) \right|^2}{\sum_{\omega=\omega_{min}}^{\omega_{max}} \left| \mathcal{D}(\omega) \right|^2} \right\}, \tag{40}$$

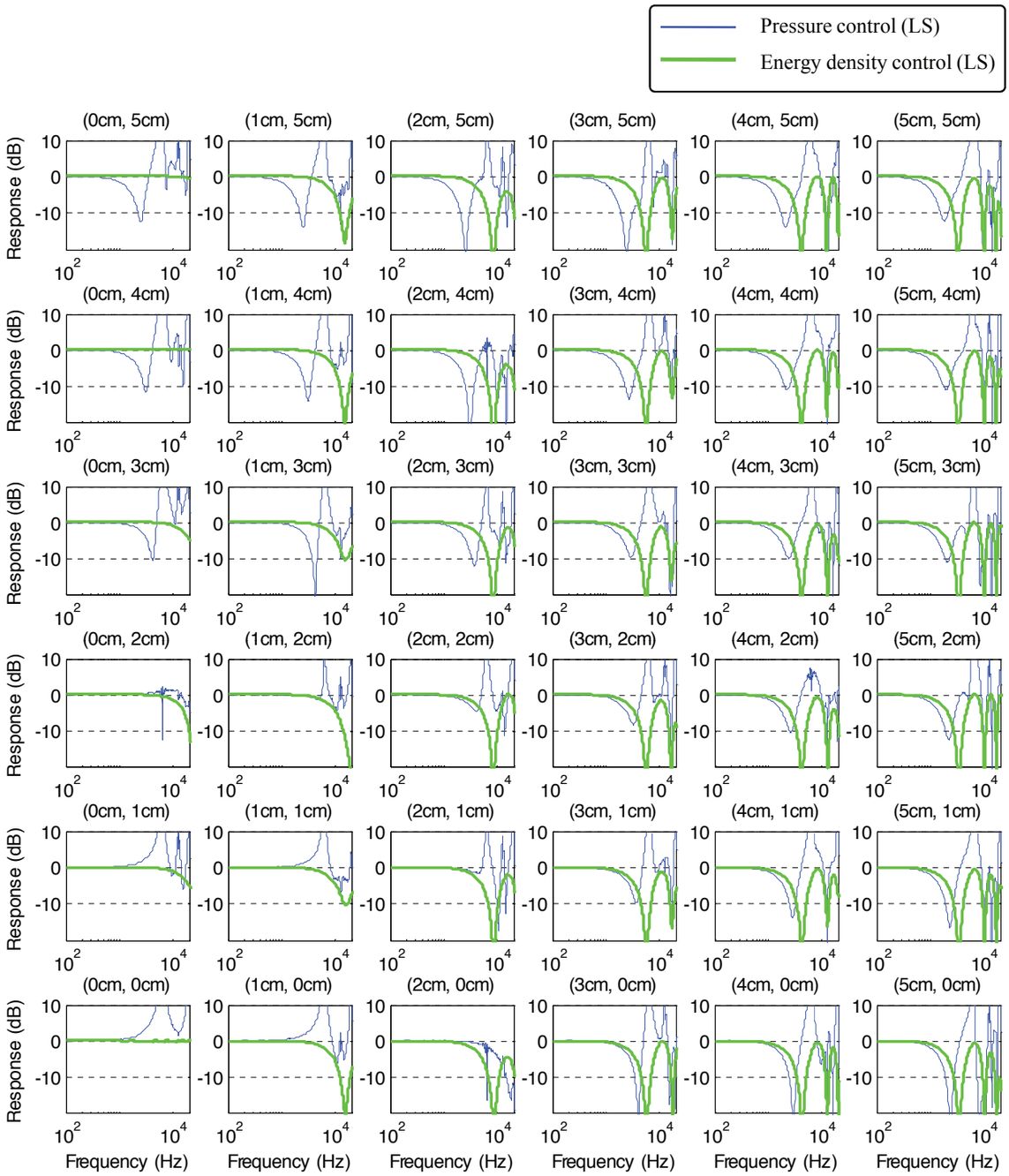

Fig. 7. The spatial extent of equalization by controlling pressure based joint LS optimization and energy density.

where ω_{min} and ω_{max} denote the minimum and maximum frequency indices of interest, respectively. In order to compare the robustness of equalization, we evaluated the pressure level in the vicinity of the control points. The equalization errors are summarized in Tables 1 and 2. Results show that the energy density control has a significantly lower equalization error than the joint LS-based squared pressure control, especially at 2 kHz where there are $7 \sim 10$ dB differences.

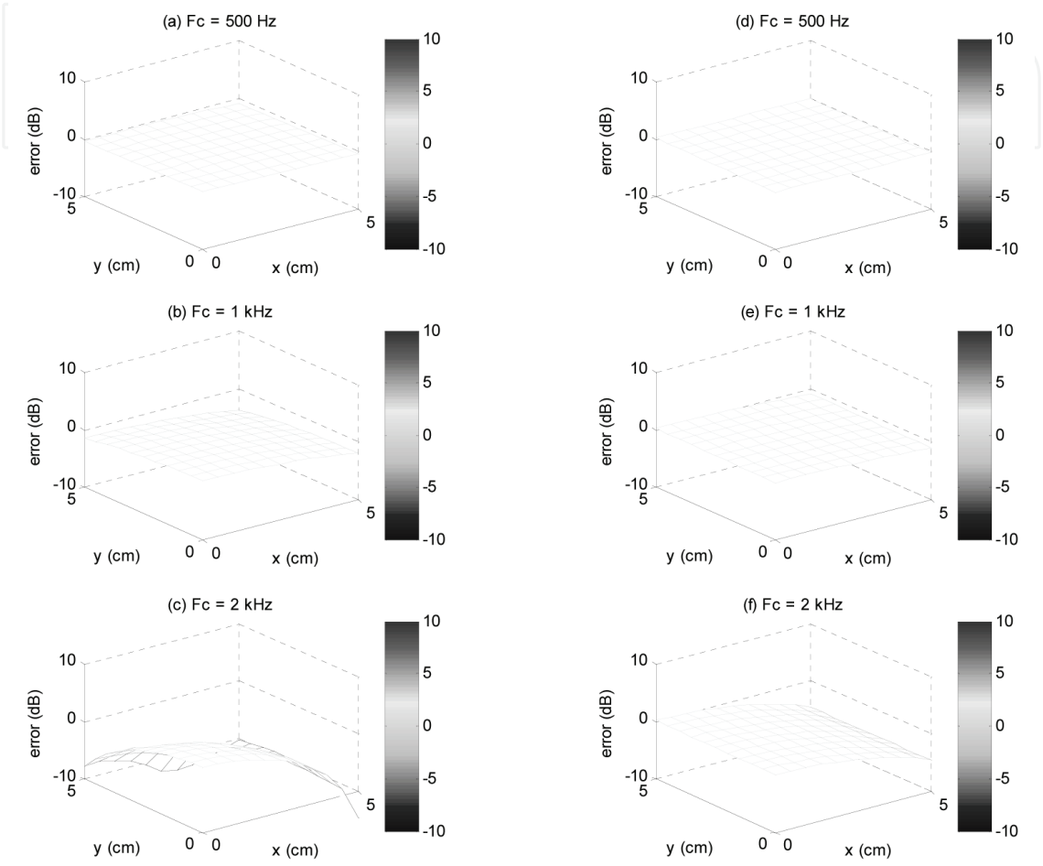

Fig. 8. A three-dimensional plot of the error surface for the pressure control (left column) and the energy density control (right column) at different center frequencies.

Finally, three-dimensional contour plots of the equalization errors are presented in Fig. 8. Fig. 8(a) and (d) show both methods have similar equalization performance at 1 kHz due to the relatively long wavelength. However, Figs. 8 (a), (b), and (c) indicate that the error of the pressure control rapidly increases as the frequency increased. On the other hand, the energy density control provides a more stable equalization zone, which implies that the energy density control can overcome the observability problem to some extent. Thus, it can be concluded that the energy density control system can provide a wider zone of equalization than the pressure control system.

4.2 Implementation consideration

It should be mentioned that it is necessary to have the acoustic velocity components to implement the energy density control system. It has been demonstrated that the

two-microphone approach yields performance which is comparable to that of ideal energy density control in the field of the active noise control system Park & Sommerfeldt (1997). Thus, it is expected that the energy density control being implemented using the two-microphone approximation maintains the robustness of room equalization observed in the previous simulations.

To examine this, we applied two microphone techniques, which were described in section 3.3 to determine the acoustic velocity along an axis. By using Eq. (28), simulations were conducted for the case of $\Delta x = 2cm$ to evaluate the performance of the two-sensor implementation. Here, l_0 and l_2 are used for estimating the velocity component for x direction and l_0 and l_4 are used for estimating the velocity component for y direction; the velocity component for z direction was not applied. The results obtained by using the ideal velocity signal and two microphone technique are shown in Fig. 9. It can be concluded that the energy density system employing the two microphone technique provides comparable performance to the control system employing the ideal velocity sensor.

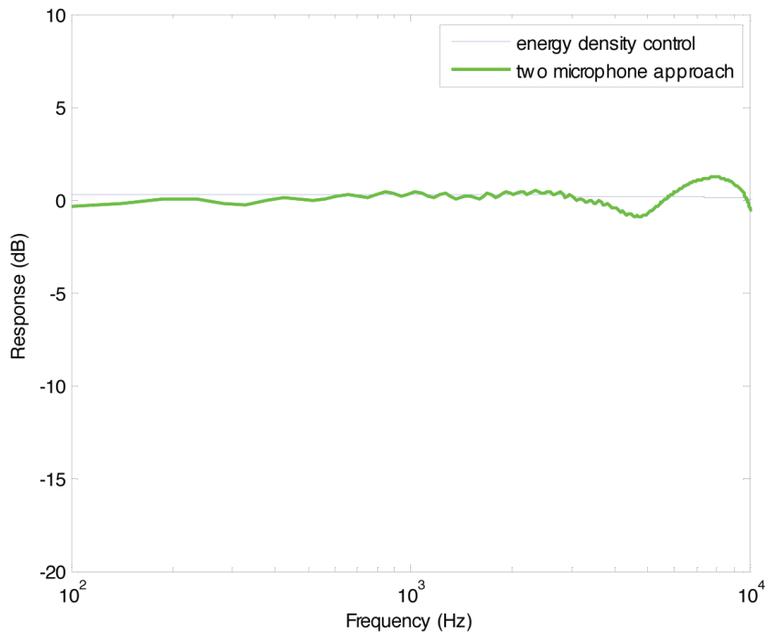

Fig. 9. The performance of the energy density control algorithm being implemented using the two microphone technique.

5. Conclusion

In this chapter, a method of designing equalization filters based on acoustic energy density was presented. In the proposed algorithm, the equalization filters are designed by minimizing the difference between the desired and produced energy densities at the control points. For the effective frequency range for the equalization, the energy density-based method provides more robust performance than the conventional squared pressure-based method. Theoretical analysis proves the robustness of the algorithm and simulation results showed that the proposed energy density-based method provides more robust performance than the conventional squared pressure-based method in terms of the spatial extent of the equalization zone.

6. References

Abe, K., Asano, F., Suzuki, Y. & Sone, T. (1997). Sound field reproduction by controlling the transfer functions from the source to multiple points in close proximity, *IEICE Trans. Fundamentals* E80-A(3): 574–581.

Elliott, S. J. & Nelson, P. A. (1989). Multiple-point equalization in a room using adaptive digital filters, *J. Audio Eng. Soc.* 37(11): 899–907.

Gardner, W. G. (1997). Head-tracked 3-d audio using loudspeakers, *Proc. IEEE Workshop on Applications of Signal Processing to Audio and Acoustics*, New Paltz, NY, USA.

Hodges, T., Nelson, P. A. & Elliot, S. J. (1990). The design of a precision digital integrator for use in an active vibration control system, *Mech. Syst. Sign. Process.* 4(4): 345–353.

Kirkeby, O., Nelson, P. A., Hamada, H. & Orduna-Bustamante, F. (1998). Fast deconvolution of multichannel systems using regularization, *IEEE Trans. on Speech and Audio Process.* 6(2): 189–195.

Mourjopoulos, J. (1994). Digital equalization of room acoustics, *J. Audio Eng. Soc.* 42(11): 884–900.

Mourjopoulos, J. & Paraskevas, M. (1991). Pole-zero modelling of room transfer functions, *J. Sound and Vib.* 146: 281–302.

Nelson, P. A., Bustamante, F. O. & Hamada, H. (1995). Inverse filter design and equalization zones in multichannel sound reproduction, *IEEE Trans. on Speech and Audio Process.* 3(3): 185–192.

Nelson, P. A., Hamada, H. & Elliott, S. J. (1992). Adaptive inverse filters for stereophonic sound reproduction, *IEEE Trans. on Signal Process.* 40(7): 1621–1632.

Park, Y. C. & Sommerfeldt, S. D. (1997). Global control of broadband noise fields using energy density control, *J. Acoust. Soc. Am.* 101: 350–359.

Parkins, J. W., Sommerfeldt, S. D. & Tichy, J. (2000). Narrowband and broadband active control in an enclosure using the acoustic energy density, *J. Acoust. Soc. Am.* 108(1): 192–203.

Rao, H. I. K., Mathews, V. J. & Park, Y.-C. (2007). A minimax approach for the joint design of acoustic crosstalk cancellation filters, *IEEE Trans. on Audio, Speech and Language Process.* 15(8): 2287–2298.

Sommerfeldt, S. D. & Nashif, P. J. (1994). An adaptive filtered-x algorithm for energy-based active control, *J. Acoust. Soc. Am.* 96(1): 300–306.

Sturm, J. F. (1999). Using sedumi 1.02, a matlab toolbox for optimization over symmetric cones, *Optim. Meth. Softw.* 11-12: 625–653.

Toole, F. E. & Olive, S. E. (1988). The modification of timbre by resonances: Perception and measurement, *J. Audio Eng. Soc.* 36: 122–141.

Ward, D. B. (2000). Joint least squares optimization for robust acoustic crosstalk cancellation, *IEEE Trans. on Speech and Audio Process.* 8(2): 211–215.

Ward, D. B. & Elko, G. W. (1999). Effect of loudspeaker position on the robustness of acoustic crosstalk cancellation, *IEEE Signal Process. Lett.* 6(5): 106–108.

Robust Control, Theory and Applications

Edited by Prof. Andrzej Bartoszewicz

ISBN 978-953-307-229-6

Hard cover, 678 pages

Publisher InTech

Published online 11, April, 2011

Published in print edition April, 2011

The main objective of this monograph is to present a broad range of well worked out, recent theoretical and application studies in the field of robust control system analysis and design. The contributions presented here include but are not limited to robust PID, H-infinity, sliding mode, fault tolerant, fuzzy and QFT based control systems. They advance the current progress in the field, and motivate and encourage new ideas and solutions in the robust control area.

How to reference

In order to correctly reference this scholarly work, feel free to copy and paste the following:

Junho Lee and Young-Cheol Park (2011). Robust Inverse Filter Design Based on Energy Density Control, Robust Control, Theory and Applications, Prof. Andrzej Bartoszewicz (Ed.), ISBN: 978-953-307-229-6, InTech, Available from: http://www.intechopen.com/books/robust-control-theory-and-applications/robust-inverse-filter-design-based-on-energy-density-control

INTECH
open science | open minds

InTech Europe

University Campus STeP Ri
Slavka Krautzeka 83/A
51000 Rijeka, Croatia
Phone: +385 (51) 770 447
Fax: +385 (51) 686 166
www.intechopen.com

InTech China

Unit 405, Office Block, Hotel Equatorial Shanghai
No.65, Yan An Road (West), Shanghai, 200040, China
中国上海市延安西路65号上海国际贵都大饭店办公楼405单元
Phone: +86-21-62489820
Fax: +86-21-62489821

© 2011 The Author(s). Licensee IntechOpen. This chapter is distributed under the terms of the Creative Commons Attribution-NonCommercial-ShareAlike-3.0 License, which permits use, distribution and reproduction for non-commercial purposes, provided the original is properly cited and derivative works building on this content are distributed under the same license.

IntechOpen

IntechOpen